

Dark matter, fine-tuning and $(g - 2)_\mu$ in the pMSSM

M. van Beekveld^{1*}, W. Beenakker², M. Schutten^{2,4}, J. de Wit²

1 Rudolf Peierls Centre for Theoretical Physics, 20 Parks Road, Oxford OX1 3PU,
United Kingdom

2 THEP, Radboud University, Heyendaalseweg 135, 6525 AJ Nijmegen, the Netherlands

3 Institute of Physics, University of Amsterdam, Science Park 904, 1018 XE Amsterdam,
the Netherlands

4 Van Swinderen Institute for Particle Physics and Gravity, University of Groningen,
9747 AG Groningen, The Netherlands

* melissa.vanbeekveld@physics.ox.ac.uk

April 29, 2021

1 Abstract

2 In this paper we analyze spectra in the phenomenological supersymmetric Stan-
3 dard Model that simultaneously result in the right dark-matter relic density
4 $\Omega_{\text{DM}} h^2$, offer an explanation for the $(g - 2)_\mu$ discrepancy Δa_μ and are minimally
5 fine-tuned. We discuss the LHC phenomenology resulting from these spec-
6 tra and the sensitivity of dark-matter direct detection experiments to these
7 spectra. We find that the latter type of experiments with sensitivity to the
8 spin-dependent dark-matter – nucleon scattering cross section $\sigma_{\text{SD,p}}$ will probe
9 all of our found solutions.

10

11 Contents

12	1 Introduction	2
13	2 The muon anomalous magnetic moment and fine-tuning in the pMSSM	3
14	2.1 Electroweak fine-tuning in the pMSSM	4
15	2.2 The muon anomalous magnetic moment	5
16	3 Analysis setup	6
17	4 Phenomenology	6
18	4.1 LHC phenomenology for the funnel regimes	8
19	4.2 LHC phenomenology for the coannihilation regimes	9
20	4.3 LHC phenomenology for the bino-higgsino LSP	10
21	4.4 Dark-matter direct detection experiments	11
22	5 Conclusion	12
23	References	12

24

25

26 1 Introduction

27 The Large Hadron Collider (LHC) has been searching for over a decade for signs of physics
 28 that originate from beyond-the-Standard-Model (BSM) scenarios, including searches for
 29 signals that originate from supersymmetric (SUSY) particle production. These high-energy
 30 searches are complemented by low-energy experiments such as dark-matter (DM) exper-
 31 iments, or experiments that search for small deviations in known Standard-Model (SM)
 32 processes from their SM prediction. In the former category, the XENON1T [1,2], PandaX-
 33 II [3,4] and PICO [5–7] experiments provide limits on the DM-nucleus scattering cross
 34 section, whereas the Planck collaboration provides a precise measurement of the DM relic
 35 abundance [8]. In the latter category, the anomalous magnetic moment of the muon $(g-2)_\mu$
 36 plays an important role. There is a long-standing discrepancy between the experimental
 37 result [9–11] and the SM prediction for the muon anomalous magnetic moment. The
 38 latter is composed of quantum-electrodynamic, weak, hadronic vacuum-polarization, and
 39 hadronic light-by-light contributions, and reads [12–33]

$$a_\mu^{\text{SM}} = \frac{(g-2)_\mu}{2} = 116\,591\,810(43) \times 10^{-11}, \quad (1)$$

40 where the value between parentheses represents the theoretical uncertainty. The improved
 41 experimental results obtained at Fermilab [34–37], combined with the Brookhaven result [9–
 42 11] read

$$a_\mu^{\text{exp}} = 116\,592\,061(41) \times 10^{-11}, \quad (2)$$

43 showing that the deviation is now

$$\Delta a_\mu = a_\mu^{\text{exp}} - a_\mu^{\text{SM}} = 251(59) \times 10^{-11}. \quad (3)$$

44 An independent experiment with different techniques than those employed by the Fermilab
 45 experiment is being constructed at J-PARC [38,39].

46 The Minimal Supersymmetric Standard Model (MSSM) with R -parity conservation pre-
 47 dicta a DM candidate and can simultaneously provide an explanation for the $(g-2)_\mu$
 48 discrepancy¹. Furthermore, the MSSM provides a solution to the fine-tuning (FT) prob-
 49 lem in the Higgs sector that any BSM model introduces, even after taking into account
 50 the constraints on colored sparticles originating from the LHC. It is clear that for a rich
 51 model such as the MSSM, the interplay between the various experimental results is of
 52 crucial importance. In this context, the interplay between the LHC limits and the $(g-2)_\mu$
 53 discrepancy has been studied in e.g. Ref. [41–48]. DM direct detection (DMDD) searches
 54 are complementary in regions of the MSSM parameter space where the LHC has little
 55 sensitivity, for example in compressed regions. Papers that explore the DM implications of
 56 spectra that explain the $(g-2)_\mu$ discrepancy include Refs. [47–52], where the relic density
 57 requirement is not always taken into account. Likelihood analyses or global fits, where all
 58 experimental data that constrain the MSSM parameter space are taken into account, have
 59 been performed in e.g. Ref. [52–58]. The degree of FT in constrained models that explain
 60 the $(g-2)_\mu$ discrepancy is studied in [59,60], whereas the role of FT in spectra with the
 61 right DM properties is studied in Ref. [61–65].

62 In this work we perform for the first time a study of the phenomenology of the MSSM
 63 that simultaneously accounts for the DM relic abundance and the observed discrepancy

¹A simultaneous explanation of the muon and electron anomalous magnetic moments in the MSSM context is provided in Ref. [40].

64 of $(g - 2)_\mu$, that includes all DMDD and LHC limits, and that constrains the model-
 65 parameter space to models that are minimally fine-tuned. The paper is structured as
 66 follows. In Section 2 we introduce our notation, the muon anomalous magnetic moment,
 67 and the electroweak fine-tuning measure. In Section 3 we explain the set-up of our analy-
 68 sis. In Section 4 we explore the phenomenology of the viable spectra, and in Section 5 we
 69 present our conclusions.

70 2 The muon anomalous magnetic moment and fine-tuning in 71 the pMSSM

72 Instead of exploring the full MSSM with 105 free parameters, we focus on the phenomeno-
 73 logical MSSM (pMSSM) [66], which has 19 free parameters. In this phenomenologically
 74 motivated pMSSM one requires that the first and second generation squark and slep-
 75 ton masses are degenerate, that the trilinear couplings of the first and second generation
 76 sfermions are set to zero (leaving only those of the third generation, A_t , A_b and A_τ), and
 77 that no new sources of CP violation are introduced. In addition one assumes that all
 78 sfermion mass matrices are diagonal. The sfermion soft-masses are then described by the
 79 first and second generation squark masses $m_{\tilde{Q}_1}$, $m_{\tilde{u}_R}$ and $m_{\tilde{d}_R}$, the third generation squark
 80 masses $m_{\tilde{Q}_3}$, $m_{\tilde{t}_R}$ and $m_{\tilde{b}_R}$, the first and second generation of slepton masses $m_{\tilde{L}_1}$ and $m_{\tilde{e}_R}$,
 81 and the third generation of slepton masses $m_{\tilde{L}_3}$ and $m_{\tilde{\tau}_R}$. The Higgs sector is described by
 82 the ratio of the Higgs vacuum expectation values $\tan \beta$ and the soft Higgs masses m_{H_u} and
 83 m_{H_d} . Instead of these parameters, it is customary to use the higgsino mass parameter μ
 84 and the mass m_A of the pseudoscalar Higgs boson as free parameters. The gaugino sector
 85 consists of the bino (\tilde{B}), wino (\tilde{W}) and gluino with their mass parameters $M_1(= |M_1|)$,
 86 $M_2(= |M_2|)$ and $M_3(= |M_3|)$.

87 As a result of electroweak symmetry breaking (EWSB), the gaugino and the higgsino in-
 88 teraction eigenstates mix into mass eigenstates, called neutralinos and charginos. The
 89 neutralinos, denoted by $\tilde{\chi}_i^0$ with $i = 1, \dots, 4$, are the neutral mass eigenstates of the bino,
 90 wino and higgsino interaction eigenstates. The neutralinos are ordered by increasing mass,
 91 with $\tilde{\chi}_1^0$ the lightest neutralino. Given the constraints from DMDD experiments on sneu-
 92 trino DM, we take the lightest neutralino as lightest-supersymmetric particle (LSP), which
 93 makes it our DM candidate. Depending on the exact values of M_1 , M_2 and $|\mu|$, this lightest
 94 mass eigenstate can be mostly bino-like (if M_1 is smallest), wino-like (if M_2 is smallest)
 95 or higgsino-like (if $|\mu|$ is smallest). The amount of bino, wino and higgsino mixing of the
 96 lightest neutralino is given by N_{11} , N_{12} and $\sqrt{N_{13}^2 + N_{14}^2}$, where N_{ij} are the entries of the
 97 matrix that diagonalizes the neutralino mass matrix. In the basis of $(\tilde{B}, \tilde{W}^0, \tilde{H}_d^0, \tilde{H}_u^0)$, this
 98 mass matrix is given by

$$M_{\tilde{\chi}^0} = \begin{pmatrix} M_1 & 0 & -c_\beta s_{\theta_W} M_Z & s_\beta s_{\theta_W} M_Z \\ 0 & M_2 & c_\beta c_{\theta_W} M_Z & -s_\beta c_{\theta_W} M_Z \\ -c_\beta s_{\theta_W} M_Z & c_\beta c_{\theta_W} M_Z & 0 & -\mu \\ s_\beta s_{\theta_W} M_Z & -s_\beta c_{\theta_W} M_Z & -\mu & 0 \end{pmatrix}, \quad (4)$$

99 with $s_x \equiv \sin x$, $c_x \equiv \cos x$, and the ratio of the SM W - and Z -boson masses being denoted
 100 by $\cos \theta_W = M_W/M_Z$.

101 The charginos, denoted by $\tilde{\chi}_i^\pm$ with $i = 1, 2$, are the charged mass eigenstates of the
 102 wino and higgsino interaction eigenstates, with $\tilde{\chi}_1^\pm$ the lightest chargino. In the basis of

103 $(\widetilde{W}^\pm, \widetilde{H}_{u/d}^\pm)$, their mass matrix at tree level reads

$$M_{\widetilde{\chi}^\pm} = \begin{pmatrix} M_2 & \sqrt{2}c_\beta c_{\theta_W} M_Z \\ \sqrt{2}s_\beta c_{\theta_W} M_Z & \mu \end{pmatrix}. \quad (5)$$

104 The composition of the lightest chargino is predominantly higgsino when $|\mu| < M_2$, pre-
105 dominantly wino when $M_2 < |\mu|$, or a mixture when the two gaugino parameters are close
106 in value.

107 2.1 Electroweak fine-tuning in the pMSSM

108 The EWSB conditions link M_Z to the input parameters via the minimization of the scalar
109 potential of the Higgs fields. The resulting equation at one loop is [67, 68]

$$\frac{M_Z^2}{2} = \frac{m_{H_d}^2 + \Sigma_d^d - (m_{H_u}^2 + \Sigma_u^u) \tan^2 \beta}{\tan^2 \beta - 1} - \mu^2, \quad (6)$$

110 where the two effective potential terms Σ_u^u and Σ_d^d denote the one-loop corrections to
111 the soft SUSY breaking Higgs masses (explicit expressions are shown in the appendix of
112 Ref. [68]). In order to obtain the observed value of $M_Z = 91.2$ GeV, one needs some degree
113 of cancellation between the SUSY parameters appearing in Eq. (6). If small relative changes
114 in the SUSY parameters will result in a distinctly different value of M_Z , the considered
115 spectrum is said to be fine-tuned, as then a large degree of cancellation is needed to obtain
116 the right value of M_Z . FT measures aim to quantify this sensitivity of M_Z to the SUSY
117 input parameters.

118 The electroweak (EW) FT measure [69, 70] is an agnostic approach to the computation of
119 fine-tuning. We take this approach because a generic broken minimal SUSY theory has
120 two relevant energy scales: a high-scale one at which SUSY breaking takes place, and a
121 low-scale one (M_{SUSY}) where the resulting SUSY particle spectrum is situated and the
122 EWSB conditions must be satisfied. We do not know which and how many fundamental
123 parameters exist for a possible high-scale theory. The EW FT measure does not take such
124 underlying high-scale model assumptions into account for its computation. The EW FT
125 measure (Δ_{EW}) parameterizes how sensitive M_Z is to variations in each of the coefficients
126 C_i , which are evaluated at M_Z . It is defined as

$$\Delta_{\text{EW}} \equiv \max_i \left| \frac{C_i}{M_Z^2/2} \right|, \quad (7)$$

127 where the C_i are

$$C_{m_{H_d}} = \frac{m_{H_d}^2}{\tan^2 \beta - 1}, \quad C_{m_{H_u}} = \frac{-m_{H_u}^2 \tan^2 \beta}{\tan^2 \beta - 1}, \quad C_\mu = -\mu^2,$$

$$C_{\Sigma_d^d} = \frac{\max(\Sigma_d^d)}{\tan^2 \beta - 1}, \quad C_{\Sigma_u^u} = \frac{-\max(\Sigma_u^u) \tan^2 \beta}{\tan^2 \beta - 1}.$$

128 The tadpole contributions Σ_u^u and Σ_d^d contain a sum of different contributions. These
129 contributions are computed individually and the maximum contribution is used to compute
130 the $C_{\Sigma_u^u}$ and $C_{\Sigma_d^d}$ coefficients. We will use an upper bound of $\Delta_{\text{EW}} < 100$ (implying no
131 worse than $\mathcal{O}(1\%)$ fine-tuning on the mass of the Z -boson) to determine whether a given
132 set of MSSM parameters is fine-tuned, and use the code from Ref. [63] to compute the
133 measure.

134 Using this measure, one generically finds that minimally fine-tuned scenarios have low

135 values for $|\mu|$, where $\Delta_{\text{EW}} = 100$ is reached at $|\mu| \simeq 800$ GeV [63, 65, 69, 71–75]. The
 136 masses of the gluino, sbottom, stop and squarks are allowed to get large for models with
 137 low Δ_{EW} [64, 76, 77]. Therefore, we assume that the masses of these sparticles are above
 138 2.5 TeV (for the gluino), above 1.2 TeV (for the stops and bottoms) and above 2 TeV (for
 139 the squarks), such that they evade the ATLAS and CMS limits ².

140 2.2 The muon anomalous magnetic moment

141 In the pMSSM, one-loop contributions to a_μ arise from diagrams with a chargino-sneutrino
 142 or neutralino-smuon loop [78]. The expressions for these one-loop corrections read [79]

$$\delta a_\mu^{\tilde{\chi}^0} = \frac{m_\mu}{16\pi^2} \sum_{i=1}^4 \sum_{m=1}^2 \left[-\frac{m_\mu}{12m_{\mu m}^2} (|n_{im}^L|^2 + |n_{im}^R|^2) F_1^N \left(\frac{m_{\tilde{\chi}_i^0}^2}{m_{\mu m}^2} \right) + \frac{m_{\tilde{\chi}_i^0}}{3m_{\mu m}^2} \text{Re} [n_{im}^L n_{im}^R] F_2^N \left(\frac{m_{\tilde{\chi}_i^0}^2}{m_{\mu m}^2} \right) \right], \quad (8)$$

$$\delta a_\mu^{\tilde{\chi}^\pm} = \frac{m_\mu}{16\pi^2} \sum_{k=1}^2 \left[\frac{m_\mu}{12m_{\tilde{\nu}_\mu}^2} (|c_k^L|^2 + |c_k^R|^2) F_1^C \left(\frac{m_{\tilde{\chi}_k^\pm}^2}{m_{\tilde{\nu}_\mu}^2} \right) + \frac{2m_{\tilde{\chi}_k^\pm}}{3m_{\tilde{\nu}_\mu}^2} \text{Re} [c_k^L c_k^R] F_2^C \left(\frac{m_{\tilde{\chi}_k^\pm}^2}{m_{\tilde{\nu}_\mu}^2} \right) \right] \quad (9)$$

143 with m_μ the muon mass, $m_{\tilde{\mu}_m}$ the first or second smuon mass, $m_{\tilde{\nu}_\mu}$ the muon sneutrino
 144 mass, i , m and k the indices for the neutralinos, smuons and charginos and the couplings

$$n_{im}^R = \sqrt{2}g_1 N_{i1} X_{m2} + y_\mu N_{i3} X_{m1}, \quad n_{im}^L = \frac{1}{\sqrt{2}} (g_2 N_{i2} + g_1 N_{i1}) X_{m1}^* - y_\mu N_{i3} X_{m2}^* \quad (10)$$

$$c_k^R = y_\mu U_{k2}, \quad c_k^L = -g_2 V_{k1}. \quad (11)$$

145 The down-type muon Yukawa coupling is denoted by $y_\mu = g_2 m_\mu / (\sqrt{2} M_W \cos \beta)$, and the
 146 SU(2) and U(1) gauge couplings are g_2 and g_1 . The matrices N and U , V diagonalize
 147 the neutralino and chargino mass matrices (Eq. (4), (5)), while the unitary matrix X
 148 diagonalizes the smuon mass matrix M_μ^2 , which reads for the pMSSM in the $(\tilde{\mu}_L, \tilde{\mu}_R)$ basis

$$M_\mu^2 = \begin{pmatrix} m_{L_1}^2 + \left(s_{\theta_W}^2 - \frac{1}{2} \right) M_Z^2 \cos(2\beta) & -m_\mu \mu \tan \beta \\ -m_\mu \mu \tan \beta & m_{e_R}^2 - s_{\theta_W}^2 M_Z^2 \cos(2\beta) \end{pmatrix}. \quad (12)$$

150 The loop functions $F_{1,2}^N$ and $F_{1,2}^C$ can be found in Ref. [79]. They are normalized such that
 151 $F_{1,2}^{N,C}(x=1) = 1$, and go to zero for $x \rightarrow \infty$.

152 At two-loop, the numerical values of the various contributions differ considerably. The
 153 photonic Barr-Zee diagrams are the source of the largest possible two-loop contribution.
 154 Here a Higgs boson and a photon connect to either a chargino or sfermion loop [80] ³.

155 As one can see in the expressions above, the chargino-sneutrino and neutralino-smuon
 156 contributions are controlled by M_1 , M_2 , $\tan \beta$ and μ (through $m_{\tilde{\chi}_i^0}$ and $m_{\tilde{\chi}_k^\pm}$), as well as
 157 $m_{\tilde{L}_1}$ and $m_{\tilde{e}_R}$ (through $m_{\tilde{\mu}_m}$ and $m_{\tilde{\nu}_\mu}$). They are enhanced when $\tan \beta$ grows large and
 158 when simultaneously light ($\mathcal{O}(100)$ GeV) neutralinos/charginos and smuons/sneutrinos
 159 exist in the sparticle spectrum. The Barr-Zee diagrams are enhanced by large values of
 160 $\tan \beta$, small values of m_A and large Higgs-sfermion couplings. In general, the one-loop
 161 chargino-sneutrino contribution dominates over the neutralino-slepton contribution [79],

²Note that those limits are shown to be significantly less stringent for MSSM spectra with rich sparticle decays, see e.g. Ref. [58].

³Two-loop corrections from sfermion loops contribute with a few percent here as well, since we assume heavy squark masses [81, 82].

162 unless there is a large smuon left-right mixing induced by a sizable value for μ [83]. These
 163 latter spectra will however result in slightly higher FT values, which is a direct consequence
 164 of a higher value of $|\mu|$.

165 3 Analysis setup

166 To create the SUSY spectra we use SOFTSUSY 4.0 [84], the Higgs mass is calculated using
 167 FeynHiggs 2.14.2 [85–89], and SUSYHIT [90] is used to calculate the decay of the SUSY
 168 and Higgs particles. Vevacious [91–93] is used to check that the models have at least a
 169 meta-stable minimum state that has a lifetime that exceeds that of our universe and that
 170 this state is not color/charge breaking ⁴. We use SUSY-AI [94] and SMODELS [95–99]
 171 to determine the LHC exclusion of a model point. LHC cross sections for sparticle pro-
 172 duction at NLO accuracy are calculated using Prospino [100]. HIGGSBOUNDS 5.1.1 is
 173 used to determine whether the SUSY models satisfy the LEP, Tevatron and LHC Higgs
 174 constraints [101–108]. MICROMEAS 5.2.1 [109–114] is used to compute the DM relic
 175 density ($\Omega_{\text{DM}}h^2$), the present-day velocity-weighted annihilation cross section ($\langle\sigma v\rangle$) and
 176 the spin-dependent and spin-independent dark-matter–nucleon scattering cross sections
 177 ($\sigma_{\text{SD,p}}$ and $\sigma_{\text{SI,p}}$). For DM indirect detection we only consider the limit on $\langle\sigma v\rangle$ stemming
 178 from the observation of gamma rays originating from dwarf galaxies, which we implement
 179 as a hard cut on each of the channels reported on the last page of Ref. [115]. The current
 180 constraints on the dark-matter–nucleon scattering cross sections originating from various
 181 dark matter direct detection (DMDD) experiments are determined via MICROMEAS,
 182 while future projections of constraints are determined via DDALC 2.0.0 [116]. Flavor ob-
 183 servables are computed with SuperIso 4.1 [117, 118], while the muon anomalous magnetic
 184 moment and its theoretical uncertainty is determined with GM2Calc [81, 119–121].
 185 We use the Gaussian particle filter [122] to search the pMSSM parameter space for in-
 186 teresting areas. The lightest SM-like Higgs boson is required to be in the mass range of
 187 $122 \text{ GeV} \leq m_h \leq 128 \text{ GeV}$. Spectra that do not satisfy the LHC bounds on sparticle
 188 masses, branching fractions of B/D -meson decays, the DMDD, or DM indirect detection
 189 bounds are removed. Our spectra are furthermore required to satisfy the LEP limits on
 190 the masses of the charginos, light sleptons and staus ($m_{\tilde{\chi}_1^\pm} > 103.5 \text{ GeV}$, $m_{\tilde{\tau}^\pm} > 90 \text{ GeV}$
 191 and $m_{\tilde{\nu}_\tau} > 85 \text{ GeV}$) [123, 124], and the constraints on the invisible and total width of the
 192 Z -boson ($\Gamma_{Z,\text{inv}} = 499.0 \pm 1.5 \text{ MeV}$ and $\Gamma_Z = 2.4952 \pm 0.0023 \text{ GeV}$) [125].

193 4 Phenomenology

194 We assume that the DM abundance is determined by thermal freeze-out and require that
 195 the lightest neutralino saturates $\Omega_{\text{DM}}h^2$ with the observed value of 0.12 [8] within 0.03 to
 196 allow for a theoretical uncertainty on the relic-density calculation. As shown above, the
 197 mass eigenstate of the DM particle is a mixture of bino, wino and higgsino interaction
 198 eigenstates. To obtain the correct relic density in the pMSSM with a pure state, one
 199 can either have a higgsino with a mass of $m_{\tilde{\chi}_1^0} \simeq 800 \text{ GeV}$ or a wino with $m_{\tilde{\chi}_1^0} \simeq 2.5 \text{ TeV}$.
 200 Spectra that saturate the relic density with lower DM masses necessarily are predominantly
 201 bino-like, mixed with higgsino/wino components. Negligible higgsino/wino components are
 202 found in so-called funnel regions [126, 127], i.e. regions where the mass of the DM particle is
 203 roughly half of the mass of the Z boson, SM-like Higgs boson or heavy Higgs boson. In such

⁴These scenarios appear in the $(g-2)_\mu$ context for large $\mu \tan\beta$, see e.g. Ref. [83].

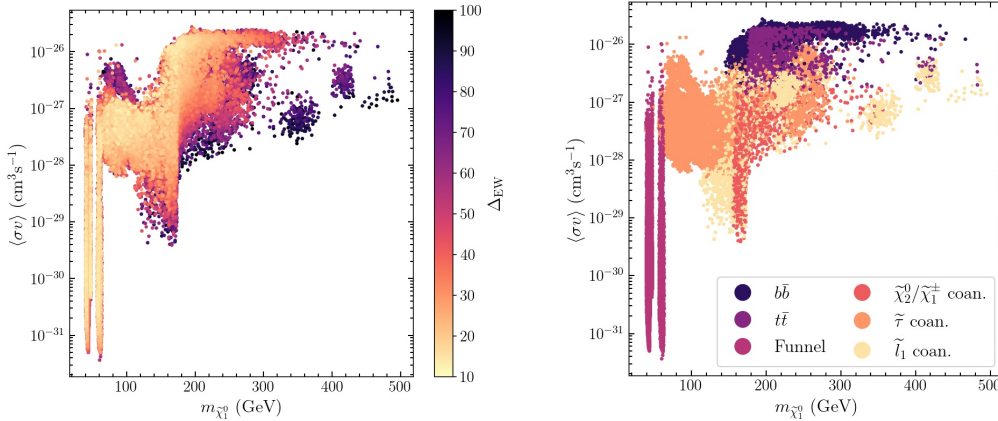


Figure 1: The mass of the DM particle ($m_{\tilde{\chi}_1^0}$) vs the velocity-weighted annihilation cross section ($\langle\sigma v\rangle$). The value of Δ_{EW} is shown as a color code on the left, where the points are ordered such that spectra with lower values of Δ_{EW} lie on top of those with higher values of Δ_{EW} . On the right we show the dominant early-universe annihilation process that contributes to the value of $\Omega_{DM}h^2$. In both plots, we only show points that satisfy all experimental constraints, and have $133 \times 10^{-11} < \Delta a_\mu < 369 \times 10^{-11}$, allowing for a 2σ uncertainty.

204 a scenario, the mass of the neutralino can even get below 100 GeV with $M_1 < 100$ GeV, and
 205 in particular the early-universe DM annihilation cross section is enhanced for $m_{\tilde{\chi}_1^0} \simeq m_h/2$
 206 and $M_Z/2$. Moreover, spectra with another particle close in mass to the LSP can satisfy
 207 the relic density constraint without having a large wino/higgsino component too, due to
 208 the co-annihilation mechanism [128].

209 The case where the lightest neutralino is predominantly wino-like results in a fine-tuned
 210 spectrum: to obtain the right relic density $M_2 \simeq 2.5$ TeV for a pure wino, so $|\mu| >$
 211 2.5 TeV in that scenario. Secondly, such high LSP neutralino masses do not give a large
 212 enough contribution to Δa_μ , since the other sparticle masses have to exceed this LSP
 213 mass. The pure-higgsino solutions do not allow for an explanation of Δa_μ [51] either.
 214 Therefore our solutions, as shown in Fig. 1, feature predominantly bino-like LSPs. Due to
 215 the combined Δa_μ constraint (requiring high $\tan\beta$), DMDD limits and the FT requirement,
 216 the composition has a small higgsino component ($< 20\%$) and a negligible wino component.
 217 The second-to-lightest neutralino and the lightest chargino are either wino-like, higgsino-
 218 like, or mixed wino-higgsino states. It might be surprising to see that spectra with bino-
 219 higgsino LSPs are allowed to have wino-like $\tilde{\chi}_2^0/\tilde{\chi}_1^\pm$. Such configurations can however be
 220 found in spectra for which M_1 , M_2 and $|\mu|$ are all of $\mathcal{O}(100)$ GeV with M_2 being smaller
 221 than $|\mu|$, and that have moderate to large values of $\tan\beta$ ($10 \lesssim \tan\beta \lesssim 20$). From Eq. (4)
 222 one may infer that for such spectra, little mixing can take place between the bino and
 223 wino. This results in negligible wino components of the LSP, whereas $\tilde{\chi}_1^\pm$ and $\tilde{\chi}_2^0$ can be
 224 predominantly wino-like. Moreover, decreasing $|\mu|$ for such models will not only result in
 225 a higher higgsino-component, but counter-intuitively also in a *higher* wino component of
 226 the LSP, while the wino component of $\tilde{\chi}_1^\pm$ and $\tilde{\chi}_2^0$ then *decreases*. Because of these higher
 227 wino/higgsino components of the LSP, such scenarios result in larger values of $\sigma_{SI,p}$ and
 228 $\sigma_{SD,p}$. Therefore, decreasing $|\mu|$ for these scenarios is limited by the constraints imposed
 229 by the DMDD experiments. The spectra where $\tilde{\chi}_1^\pm$ and $\tilde{\chi}_2^0$ are predominantly higgsino-like
 230 are typically difficult to probe at the LHC due to low production cross sections compared
 231 to the pure wino $\tilde{\chi}_1^\pm/\tilde{\chi}_2^0$ case.

232 In Fig. 1 we show the spectra that survive all constraints and have $\Delta_{EW} < 100$. Lower
 233 values for Δ_{EW} are generally found for lower DM masses. The mass of the DM particle
 234 does not exceed 500 GeV, which is a direct result of the combined requirements of having

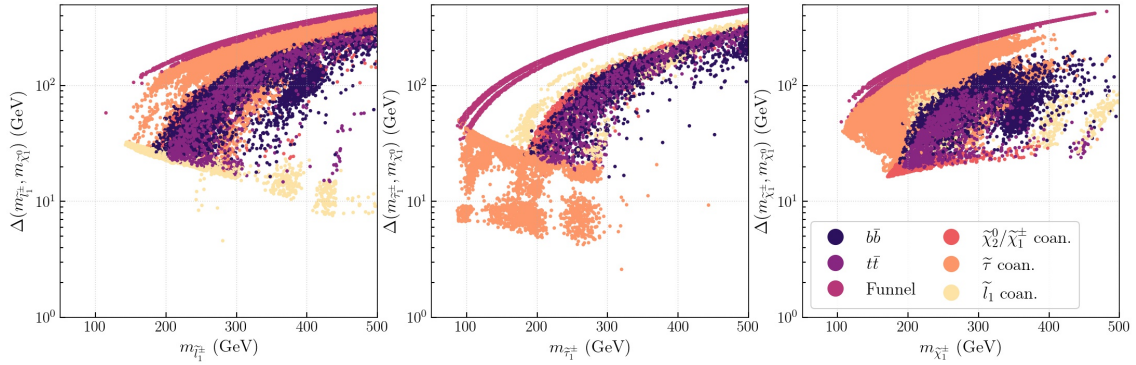


Figure 2: The mass difference between the DM particle and the lightest chargino (left), lightest smuon (middle) and lightest stau (right) versus the mass of the heavier particle. The color code represents the dominant early-universe annihilation channel.

235 $\Delta_{\text{EW}} < 100$ and a sufficiently high contribution to Δa_μ . The lowest-obtained value is
 236 $\Delta_{\text{EW}} = 12.3$. From the right-hand side of Fig. 1, we can distinguish three different type of
 237 DM early-universe annihilation mechanisms: the funnel regions, the coannihilation regions
 238 and the bino-higgsino solution (indicated with $b\bar{b}$ and $t\bar{t}$). As the LHC phenomenology of
 239 these three early-universe annihilation regimes can be quite different, we now discuss them
 240 one-by-one.

241 4.1 LHC phenomenology for the funnel regimes

242 We start with the funnel regions, of which there are two in our spectra ⁵. The first one
 243 centers around $m_{\tilde{\chi}_1^0} \simeq 40$ GeV, which is slightly less than $M_Z/2$. This can be explained
 244 as follows. The velocities of the DM particles were much higher in the early universe
 245 than what they are in the present-day universe. This means that DM annihilations via
 246 s-channel Z exchanges could happen on-resonance in the early universe, whereas in the
 247 present-day universe these exchanges only happen off-resonance. This also explains the
 248 fact that the value for $\langle\sigma v\rangle$ is allowed to get orders of magnitude smaller than the value
 249 that one usually expects for a thermal relic (around $\langle\sigma v\rangle = 3 \cdot 10^{-26} \text{ cm}^3\text{s}^{-1}$ for a DM mass
 250 of 100 GeV). These models are characterized by small wino/higgsino components of the
 251 LSP - otherwise the early-universe annihilation would be too efficient, resulting in a too-
 252 low value of $\Omega_{\text{DM}}h^2$. The second funnel region is centered around $m_{\tilde{\chi}_1^0} \simeq 60$ GeV, slightly
 253 less than $m_h/2$. These DM particles annihilated in the early universe predominantly via
 254 s-channel SM-like Higgs exchanges. No solutions are found for spectra with DM masses
 255 in-between the two funnel regions. Here, the wino/higgsino component necessarily needs
 256 to increase to satisfy the $\Omega_{\text{DM}}h^2$ requirement, and these spectra are excluded by DMDD
 257 experiments. The minimal value of Δ_{EW} for these spectra is 13.2.

258 The two funnel regimes are characterized by light ($m_{\tilde{\chi}_1^0} < 100$ GeV) bino-like LSPs. The $\tilde{\chi}_1^\pm$
 259 and $\tilde{\chi}_2^0$ are degenerate in mass. They are wino mixtures for masses around 100 – 200 GeV,
 260 while they become higgsino-like for heavier $\tilde{\chi}_1^\pm / \tilde{\chi}_2^0$ (up to $m_{\tilde{\chi}_1^\pm} / \tilde{\chi}_2^0 \simeq 500$ GeV). The
 261 mass gap between $\tilde{\chi}_1^0$ and $\tilde{\chi}_2^0$ or $\tilde{\chi}_1^\pm$ ($\Delta(m_{\tilde{\chi}_2^0}, m_{\tilde{\chi}_1^0})$ or $\Delta(m_{\tilde{\chi}_1^\pm}, m_{\tilde{\chi}_1^0})$) is at least around
 262 50 GeV, and exceeds 100 GeV for $m_{\tilde{\chi}_1^\pm} \gtrsim 150$ GeV (see Fig. 2, left panel). The masses
 263 of the sleptons are heavier than (at least) the masses of $\tilde{\chi}_2^0$ and $\tilde{\chi}_1^\pm$. Therefore, three
 264 different sorts of decays for $\tilde{\chi}_2^0$ can be identified: 1. $\tilde{\chi}_2^0 \rightarrow h\tilde{\chi}_1^0$ when $\Delta(m_{\tilde{\chi}_2^0}, m_{\tilde{\chi}_1^0}) > m_h$,
 265 2. $\tilde{\chi}_2^0 \rightarrow Z\tilde{\chi}_1^0$ when $\Delta(m_{\tilde{\chi}_2^0}, m_{\tilde{\chi}_1^0}) > M_Z$, and 3. off-shell decays when $\Delta(m_{\tilde{\chi}_2^0}, m_{\tilde{\chi}_1^0}) < M_Z$.

⁵The heavy Higgs funnel is not identified here, and will be left for future study.

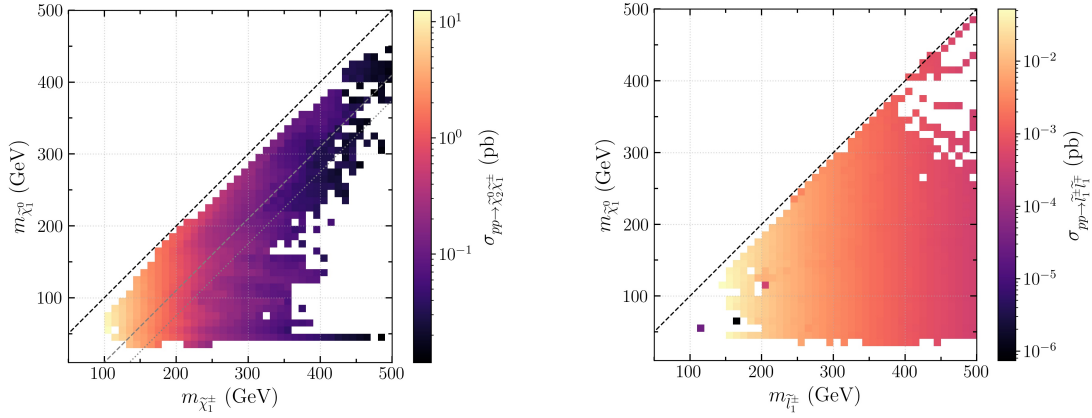


Figure 3: The mass of the DM particle versus the mass of the lightest chargino (left) and smuon (right), combined in 10 by 10 GeV bins. The average production cross section of $\sigma_{pp \rightarrow \tilde{\chi}_2^0 \tilde{\chi}_1^\pm}$ (left) and $\sigma_{pp \rightarrow \tilde{l}_1^\pm \tilde{l}_1^\mp}$ (right) is shown in color code for each bin. The dashed black line in the plot on the left-hand side shows the limit where $m_{\tilde{\chi}_2^0} = m_{\tilde{\chi}_1^\pm}$, whereas the gray dashed (dotted) lines show $m_{\tilde{\chi}_1^\pm} = m_{\tilde{\chi}_1^0} + M_Z$ ($m_{\tilde{\chi}_1^\pm} = m_{\tilde{\chi}_1^0} + m_h$). The dashed black line in the plot on the right-hand side shows $m_{\tilde{\chi}_1^0} = m_{\tilde{l}_1^\pm}$.

266 For $\tilde{\chi}_1^\pm$, there are only two sorts of decays: 1. $\tilde{\chi}_1^\pm \rightarrow W^\pm \tilde{\chi}_1^0$ when $\Delta(m_{\tilde{\chi}_1^\pm}, m_{\tilde{\chi}_1^0}) > M_W$,
 267 and 2. off-shell decays when $\Delta(m_{\tilde{\chi}_1^\pm}, m_{\tilde{\chi}_1^0}) < M_W$. Searches for $\tilde{\chi}_2^0 \tilde{\chi}_1^\pm$ production with
 268 on-shell decays of $\tilde{\chi}_2^0 \rightarrow Z \tilde{\chi}_1^0$ are most sensitive to our spectra [129–131]. In our models,
 269 whenever $\Delta(m_{\tilde{\chi}_2^0}, m_{\tilde{\chi}_1^0}) > m_h$, there exists a mixture between $\tilde{\chi}_2^0 \rightarrow h \tilde{\chi}_1^0$ and $\tilde{\chi}_2^0 \rightarrow Z \tilde{\chi}_1^0$
 270 decays. The sensitivity of the experiments drops when $\tilde{\chi}_2^0$ can decay into the SM-like Higgs
 271 boson [130, 132]. The simplified limits of the searches mentioned above assume a wino-like
 272 $\tilde{\chi}_2^0 \tilde{\chi}_1^\pm$ pair, whereas we deal with mixed wino-higgsino pairs. To recast their analysis, we
 273 show in the left panel of Fig. 3 the average cross section per 10 by 10 GeV bin for $\tilde{\chi}_2^0 \tilde{\chi}_1^\pm$
 274 production. We find that our cross sections in the regime where $M_Z < \Delta(m_{\tilde{\chi}_2^0}, m_{\tilde{\chi}_1^0}) < m_h$
 275 do not exceed the 95% confidence level (CL) limits of Ref. [130, 131]. The models
 276 with off-shell decays are slightly more constrained by the LHC experiments. Particularly
 277 Ref. [133] excludes some of our spectra in this regime that have $m_{\tilde{\chi}_1^\pm}$ up to 210 GeV and
 278 $\Delta(m_{\tilde{\chi}_2^0}, m_{\tilde{\chi}_1^0}) < 55$ GeV.

279 4.2 LHC phenomenology for the coannihilation regimes

280 The second regime is the coannihilation regime. It starts to open up at DM masses of
 281 roughly 75 GeV, as no charged sparticles (and therefore no coannihilation partners other
 282 than the sneutrino) can exist with masses below 85 GeV due to the LEP/LHC bounds.
 283 Three different types of coannihilation partners are identified: first-/second-generation
 284 sleptons, third-generation sleptons, and charginos or heavier neutralinos. Interestingly,
 285 only with the help of slepton coannihilations the DM particle can have a mass between
 286 $\mathcal{O}(70 - 150)$ GeV and still give the right $\Omega_{\text{DM}} h^2$. To obtain the right relic density in
 287 this regime without a slepton-coannihilation partner, one generally needs high higgsino
 288 fractions, which increases the value of $\sigma_{\text{SI,p}}$ beyond the exclusion limit of the DMDD
 289 experiments. The lowest values of Δ_{EW} are found in the stau-coannihilation regime
 290 ($\Delta_{\text{EW}} = 12.3$), while the first-/second-generation slepton and chargino/neutralino regimes
 291 result in lowest values $\Delta_{\text{EW}} = 14.4$ and $\Delta_{\text{EW}} = 16.4$ respectively. The coannihilation
 292 regimes are all characterized by small mass differences between the LSP and its coannihi-
 293 lation partner(s).

294 The first type of coannihilation is that of first-/second-generation sleptons (\tilde{l}_1^\pm). The com-
 295 pression between $m_{\tilde{l}_1^\pm}$ and $m_{\tilde{\chi}_1^0}$ is increased for higher LSP masses such that the right
 296 $\Omega_{\text{DM}}h^2$ can still be obtained. Spectra with $\Delta(m_{\tilde{\chi}_2^0}, m_{\tilde{\chi}_1^0}) > M_Z$ are under strong con-
 297 straints from searches for $\tilde{\chi}_2^0\tilde{\chi}_1^\pm \rightarrow \tilde{l}\tilde{l}\nu_l$ (see e.g. [132]). We explicitly remove those points
 298 from our spectra, leaving only models with $\Delta(m_{\tilde{\chi}_2^0}, m_{\tilde{\chi}_1^0}) < M_Z$. The $\tilde{\chi}_1^\pm$ and $\tilde{\chi}_2^0$ sparticles
 299 are typically higgsino-like with a small wino component, and have masses between 180 and
 300 500 GeV.

301 The second coannihilation regime is characterized by low $\tilde{\tau}_1^\pm$ masses. The masses of
 302 $\tilde{\chi}_1^\pm/\tilde{\chi}_2^0$ can still be as light as 105 GeV in this regime, where they are predominantly
 303 wino-like. The higgsino component of these particles increases when their masses in-
 304 crease, up to $m_{\tilde{\chi}_1^\pm/\tilde{\chi}_2^0} \simeq 500$ GeV. Although we have a large production cross section
 305 for the wino-like $\tilde{\chi}_1^\pm/\tilde{\chi}_2^0$ pair, these models are not constrained by the LHC experiments
 306 due to the presence of the light staus. The staus are often lighter than $\tilde{\chi}_1^\pm$ and $\tilde{\chi}_2^0$, and
 307 the searches for $\tilde{\tau}_1^\pm$ -mediated decays of $\tilde{\chi}_1^+\tilde{\chi}_1^-/\tilde{\chi}_1^\pm\tilde{\chi}_2^0$ production have no sensitivity when
 308 $\Delta(m_{\tilde{\chi}_1^0}, m_{\tilde{\tau}_1^\pm}) < 100$ GeV [134,135]. The latter holds for our spectra in the second coannihi-
 309 lation regime, since the mass differences between the LSP and $\tilde{\tau}_1^\pm$ are between 5 – 50 GeV
 310 in that case. Additionally, relatively few LHC searches for low-mass $\tilde{\tau}^\pm$ particles exist.
 311 Small $\tilde{\tau}^+\tilde{\tau}^-$ production cross sections and low signal acceptances make these searches dif-
 312 ficult, so the experiments have no constraining power in the compressed regime [136,137].
 313 *A dedicated low mass $\tilde{\tau}^\pm$ search without an assumed mass degeneracy between $\tilde{\tau}_1^\pm$ and $\tilde{\tau}_2^\pm$*
 314 *would be interesting to probe the sensitivity of the LHC to these scenarios.*

315 The last coannihilation regime has a $\tilde{\chi}_1^\pm$ or $\tilde{\chi}_2^0$ that is close in mass to the LSP. Note that
 316 although the slepton masses in these regions can be $\mathcal{O}(200)$ GeV, the results from the
 317 $\tilde{l}_{R,L}^+\tilde{l}_{R,L}^-$ searches with $\tilde{l}^\pm = \tilde{e}^\pm, \tilde{\mu}^\pm$ or $\tilde{\tau}^\pm$ (e.g. [137–139]) are not directly applicable here,
 318 as often one or more of the chargino/heavier neutralino states is lighter than the sleptons.
 319 Therefore, the slepton will not decay with a 100% branching ratio to $\tilde{\chi}_1^0l^\pm$, although this is
 320 assumed in the above-mentioned searches. Instead, in this regime, only the $\tilde{\chi}_1^\pm\tilde{\chi}_2^0$ searches
 321 are of relevance, similar to the case in the funnel region discussed above. Interestingly,
 322 although the mass compression for the slepton coannihilation regimes needs to increase to
 323 obtain the right relic density for higher DM masses, for the gaugino-coannihilation regime
 324 it instead needs to decrease. The mass compression between the LSP and wino-higgsino
 325 like $\tilde{\chi}_1^\pm/\tilde{\chi}_2^0$ sparticles is generally around 15-20 GeV, and Ref. [133] excludes our solutions
 326 with $m_{\tilde{\chi}_1^\pm}$ up to 140 – 180 GeV.

327 4.3 LHC phenomenology for the bino-higgsino LSP

328 The last regime we identify consists of bino-higgsino LSPs and is labeled with $b\bar{b}$ and $t\bar{t}$.
 329 These early-universe annihilation channels are mediated by either s-channel Z or h/H ex-
 330 changes. The $t\bar{t}$ annihilation channel opens up when $m_{\tilde{\chi}_1^0}$ becomes larger than the mass
 331 of the top quark m_t , as then the invariant mass of the two LSPs is enough to create a $t\bar{t}$
 332 pair ⁶. For the Z -exchange channel this annihilation becomes favored over the annihilation
 333 into a lighter fermion pair, since any Z -mediated annihilation of two Majorana fermions
 334 is helicity suppressed at tree level [140]. This is explained as follows. The two identical
 335 LSPs form a Majorana pair. Such a pair is even under the operation of charge-conjugation
 336 $C = (-1)^{L+S}$ with S the total spin and L the total orbital angular momentum, so L and
 337 S must either both be even, or both be odd. Taking the limit of zero velocity, as the
 338 present-day velocity of DM particles is non-relativistic, we may assume $L = 0$ and even S .

⁶The annihilation to a W^+W^- pair is possible when $m_{\tilde{\chi}_1^0} > M_W$. However, this is constrained by DMDD due to the high wino/higgsino fraction that is necessary for this channel.

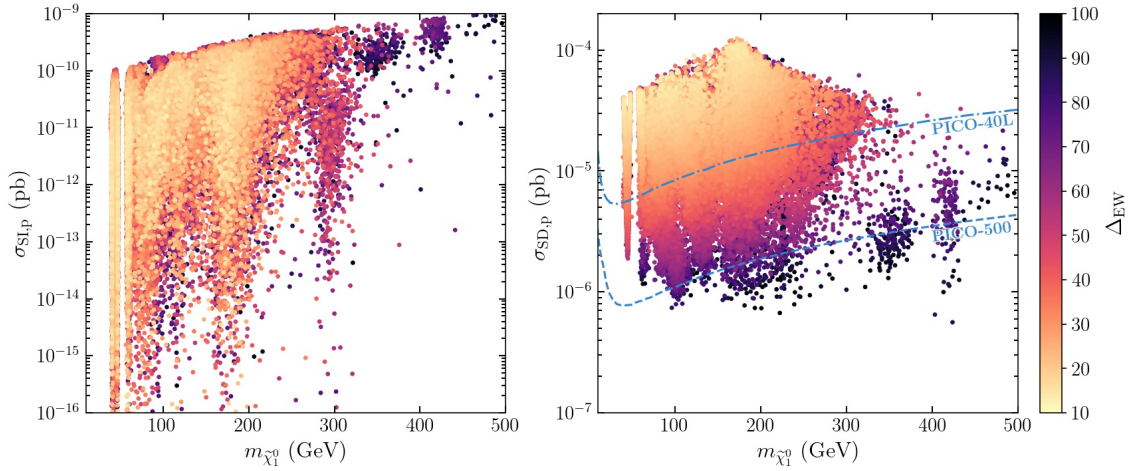


Figure 4: Right (left): The mass of the DM particle versus the spin-(in)dependent cross section $\sigma_{SD,p}$ ($\sigma_{SI,p}$). The value of Δ_{EW} is shown in color code. We also show the projected PICO-40L and PICO-500 central limits on $\sigma_{SD,p}$ [141]. The points are ordered such that those with lower values of Δ_{EW} lie on top of those with higher values.

339 The final-state fermion pair can have a total spin of $S = 1$ or $S = 0$, but only the latter is
 340 allowed for the Majorana-pair annihilation in the non-relativistic limit. For a Dirac-field
 341 pair, an $S = 0$ configuration is obtained if the fermion and anti-fermion are from different
 342 Weyl spinors: a left- and right-handed one. In the SM, a coupling with this combination
 343 only arises (at tree level) by a mass insertion. Therefore, the transition amplitude is pro-
 344 portional to the mass of the final-state fermions, and a decay to a heavier pair of fermions
 345 is generally preferred. In spectra where $\tan\beta$ is large we also see the heavy-Higgs-mediated
 346 decays to $b\bar{b}$, as the bottom-Yukawa coupling is enhanced. As can be seen in Fig. 2, in the
 347 regime of $m_{\tilde{\chi}_1^0} \gtrsim m_t$, the masses of $\tilde{\chi}_1^\pm$ and $\tilde{\chi}_2^0$ are relatively close to that of the LSP, so
 348 due to the coannihilation mechanism these spectra tend to show slightly lower values of
 349 $\langle\sigma v\rangle$ than naively would be expected.

350 The minimal value of Δ_{EW} is around 14.2 for these models. The $\tilde{\chi}_2^0$ and $\tilde{\chi}_1^\pm$ are predomi-
 351 nantly higgsino-like with masses from 180 to 500 GeV. Due to their small production cross
 352 section, the LHC searches do not have exclusion power in this regime.

353 4.4 Dark-matter direct detection experiments

354 In the previous subsections we discussed the phenomenology of the viable spectra at the
 355 LHC. We now comment on the sensitivity of DMDD experiments. The resulting values
 356 for $\sigma_{SI,p}$ and $\sigma_{SD,p}$ may be seen in Fig. 4. While the value of $\sigma_{SI,p}$ varies by over 7
 357 orders of magnitude, $\sigma_{SD,p}$ is relatively constrained. Moreover, we observe that $\sigma_{SD,p}$
 358 is directly correlated with Δ_{EW} : lower values of $\sigma_{SD,p}$ result in higher values of Δ_{EW} . This
 359 is due to the fact that the LSP in our spectra is always bino-like with a small higgsino
 360 component. The value of $\sigma_{SD,p}$ decreases with smaller higgsino fractions in the LSP, while
 361 Δ_{EW} increases since $|\mu|$ needs to increase (for a given fixed LSP mass). *For this reason,*
 362 *future DMDD experiments that probe $\sigma_{SD,p}$ will be sensitive to all our solutions, irrespective*
 363 *of the masses and compositions of the rest of the sparticle spectrum.* In Fig. 4, we indicate
 364 the projected limit of the PICO-40L and the PICO-500 experiments [141]. We observe
 365 that the latter one is sensitive to all of our solutions with $\Delta_{EW} < 62$. The LUX-ZEPLIN
 366 experiment [142] (whose projected limit is not shown in Fig. 4) will exclude all of our
 367 solutions with $\Delta_{EW} < 100$.

368 5 Conclusion

369 In this paper we have analyzed the spectra in the pMSSM that are minimally fine-tuned,
370 result in the right $\Omega_{\text{DM}}h^2$ and simultaneously offer an explanation for Δa_μ . In terms of DM
371 phenomenology, we have distinguished three interesting branches of solutions: the funnel
372 regimes, three types of coannihilation regimes, and the generic bino-higgsino solution.
373 All these solutions have in common that the LSP is predominantly bino-like with a small
374 higgsino component. Masses of the DM particle range between 39 – 495 GeV. We discussed
375 the phenomenology at the LHC for each of the regimes. The first and second regime
376 are relatively more constrained by $\tilde{\chi}_2^0\tilde{\chi}_1^\pm$ searches at the LHC (in particular by the one
377 presented in Ref. [133]) than the last regime, which is due to the lower wino-components
378 and higher masses of the $\tilde{\chi}_2^0/\tilde{\chi}_1^\pm$ sparticles that is typical in the last regime. On the other
379 hand, in particular when the coannihilation partner of the LSP is a light stau, the LHC
380 searches show little to no sensitivity to our found solutions. A dedicated low-mass $\tilde{\tau}^\pm$
381 search without an assumed mass degeneracy between $\tilde{\tau}_1^\pm$ and $\tilde{\tau}_2^\pm$ would be interesting to
382 probe the sensitivity of the LHC to these scenarios. The requirement of satisfying Δa_μ
383 excludes models with a higher-mass higgsino of around 600 GeV as the LSP, which means
384 that the value of $\sigma_{\text{SD,p}}$ is directly linked to Δ_{EW} . Therefore, DMDD experiments that
385 probe $\sigma_{\text{SD,p}}$ will ultimately be sensitive to all of our found solutions.

386 Acknowledgments

387 MvB acknowledges support from the Science and Technology Facilities Council (grant
388 number ST/T000864/1).

389 References

- 390 [1] E. Aprile *et al.*, *Dark matter search results from a one ton-year*
391 *exposure of XENON1T*, Phys. Rev. Lett. **121**(11), 111302 (2018),
392 doi:10.1103/PhysRevLett.121.111302, 1805.12562.
- 393 [2] E. Aprile *et al.*, *Constraining the spin-dependent WIMP-nucleon cross*
394 *sections with XENON1T*, Phys. Rev. Lett. **122**(14), 141301 (2019),
395 doi:10.1103/PhysRevLett.122.141301, 1902.03234.
- 396 [3] J. Xia *et al.*, *PandaX-II constraints on spin-dependent WIMP-nucleon effective*
397 *interactions*, Phys. Lett. **B792**, 193 (2019), doi:10.1016/j.physletb.2019.02.043,
398 1807.01936.
- 399 [4] A. Tan *et al.*, *Dark matter results from first 98.7 days of data from*
400 *the PandaX-II experiment*, Phys. Rev. Lett. **117**(12), 121303 (2016),
401 doi:10.1103/PhysRevLett.117.121303, 1607.07400.
- 402 [5] C. Amole *et al.*, *Dark Matter Search Results from the Complete Exposure of the*
403 *PICO-60 C₃F₈ Bubble Chamber* (2019), 1902.04031.
- 404 [6] C. Amole *et al.*, *Dark Matter Search Results from the PICO-60 C₃F₈ Bubble Cham-*
405 *ber*, Phys. Rev. Lett. **118**(25), 251301 (2017), doi:10.1103/PhysRevLett.118.251301,
406 1702.07666.

- 407 [7] C. Amole *et al.*, *Improved dark matter search results from PICO-2L Run 2*, Phys.
408 Rev. **D93**(6), 061101 (2016), doi:10.1103/PhysRevD.93.061101, 1601.03729.
- 409 [8] N. Aghanim *et al.*, *Planck 2018 results. VI. Cosmological parameters*, Astron. As-
410 trophys. **641**, A6 (2020), doi:10.1051/0004-6361/201833910, 1807.06209.
- 411 [9] G. W. Bennett *et al.*, *Final Report of the Muon E821 Anomalous Mag-
412 netic Moment Measurement at BNL*, Phys. Rev. D **73**, 072003 (2006),
413 doi:10.1103/PhysRevD.73.072003, hep-ex/0602035.
- 414 [10] G. W. Bennett *et al.*, *Measurement of the negative muon anomalous
415 magnetic moment to 0.7 ppm*, Phys. Rev. Lett. **92**, 161802 (2004),
416 doi:10.1103/PhysRevLett.92.161802, hep-ex/0401008.
- 417 [11] G. W. Bennett *et al.*, *Measurement of the positive muon anomalous magnetic moment
418 to 0.7 ppm*, Phys. Rev. Lett. **89**, 101804 (2002), doi:10.1103/PhysRevLett.89.101804,
419 [Erratum: Phys.Rev.Lett. 89, 129903 (2002)], hep-ex/0208001.
- 420 [12] G. Colangelo, M. Hoferichter and P. Stoffer, *Two-pion contribution to hadronic
421 vacuum polarization*, JHEP **02**, 006 (2019), doi:10.1007/JHEP02(2019)006, 1810.
422 00007.
- 423 [13] M. Davier, A. Hoecker, B. Malaescu and Z. Zhang, *Reevaluation of the hadronic
424 vacuum polarisation contributions to the Standard Model predictions of the muon
425 $g - 2$ and $\alpha(m_Z^2)$ using newest hadronic cross-section data*, Eur. Phys. J. C **77**(12),
426 827 (2017), doi:10.1140/epjc/s10052-017-5161-6, 1706.09436.
- 427 [14] A. Keshavarzi, D. Nomura and T. Teubner, *Muon $g-2$ and $\alpha(M_Z^2)$: a new data-based
428 analysis*, Phys. Rev. D **97**(11), 114025 (2018), doi:10.1103/PhysRevD.97.114025,
429 1802.02995.
- 430 [15] M. Hoferichter, B.-L. Hoid and B. Kubis, *Three-pion contribution to hadronic vacuum
431 polarization*, JHEP **08**, 137 (2019), doi:10.1007/JHEP08(2019)137, 1907.01556.
- 432 [16] A. Kurz, T. Liu, P. Marquard and M. Steinhauser, *Hadronic contribution to the
433 muon anomalous magnetic moment to next-to-next-to-leading order*, Phys. Lett. B
434 **734**, 144 (2014), doi:10.1016/j.physletb.2014.05.043, 1403.6400.
- 435 [17] K. Melnikov and A. Vainshtein, *Hadronic light-by-light scattering contribution to
436 the muon anomalous magnetic moment revisited*, Phys. Rev. D **70**, 113006 (2004),
437 doi:10.1103/PhysRevD.70.113006, hep-ph/0312226.
- 438 [18] G. Colangelo, M. Hoferichter, M. Procura and P. Stoffer, *Dispersion relation for
439 hadronic light-by-light scattering: two-pion contributions*, JHEP **04**, 161 (2017),
440 doi:10.1007/JHEP04(2017)161, 1702.07347.
- 441 [19] M. Hoferichter, B.-L. Hoid, B. Kubis, S. Leupold and S. P. Schneider, *Disper-
442 sion relation for hadronic light-by-light scattering: pion pole*, JHEP **10**, 141 (2018),
443 doi:10.1007/JHEP10(2018)141, 1808.04823.
- 444 [20] A. Gérardin, H. B. Meyer and A. Nyffeler, *Lattice calculation of the pion transition
445 form factor with $N_f = 2 + 1$ Wilson quarks*, Phys. Rev. D **100**(3), 034520 (2019),
446 doi:10.1103/PhysRevD.100.034520, 1903.09471.

- 447 [21] G. Colangelo, F. Hagelstein, M. Hoferichter, L. Laub and P. Stoffer, *Longitudinal*
448 *short-distance constraints for the hadronic light-by-light contribution to $(g-2)_\mu$ with*
449 *large- N_c Regge models*, JHEP **03**, 101 (2020), doi:10.1007/JHEP03(2020)101, 1910.
450 13432.
- 451 [22] G. Colangelo, M. Hoferichter, A. Nyffeler, M. Passera and P. Stoffer, *Remarks on*
452 *higher-order hadronic corrections to the muon $g-2$* , Phys. Lett. B **735**, 90 (2014),
453 doi:10.1016/j.physletb.2014.06.012, 1403.7512.
- 454 [23] P. Masjuan and P. Sanchez-Puertas, *Pseudoscalar-pole contribution to the*
455 *$(g_\mu - 2)$: a rational approach*, Phys. Rev. D **95**(5), 054026 (2017),
456 doi:10.1103/PhysRevD.95.054026, 1701.05829.
- 457 [24] T. Blum, N. Christ, M. Hayakawa, T. Izubuchi, L. Jin, C. Jung and C. Lehner,
458 *Hadronic Light-by-Light Scattering Contribution to the Muon Anomalous Mag-*
459 *netic Moment from Lattice QCD*, Phys. Rev. Lett. **124**(13), 132002 (2020),
460 doi:10.1103/PhysRevLett.124.132002, 1911.08123.
- 461 [25] J. Prades, E. de Rafael and A. Vainshtein, *The Hadronic Light-by-Light Scattering*
462 *Contribution to the Muon and Electron Anomalous Magnetic Moments*, Adv. Ser.
463 Direct. High Energy Phys. **20**, 303 (2009), doi:10.1142/9789814271844_0009, 0901.
464 0306.
- 465 [26] M. Davier, A. Hoecker, B. Malaescu and Z. Zhang, *A new evaluation of the hadronic*
466 *vacuum polarisation contributions to the muon anomalous magnetic moment and to*
467 *$\alpha(\mathbf{m}_Z^2)$* , Eur. Phys. J. C **80**(3), 241 (2020), doi:10.1140/epjc/s10052-020-7792-2,
468 [Erratum: Eur.Phys.J.C 80, 410 (2020)], 1908.00921.
- 469 [27] A. Keshavarzi, D. Nomura and T. Teubner, *$g-2$ of charged leptons, $\alpha(M_Z^2)$*
470 *, and the hyperfine splitting of muonium*, Phys. Rev. D **101**(1), 014029 (2020),
471 doi:10.1103/PhysRevD.101.014029, 1911.00367.
- 472 [28] C. Gnendiger, D. Stöckinger and H. Stöckinger-Kim, *The electroweak contributions*
473 *to $(g-2)_\mu$ after the Higgs boson mass measurement*, Phys. Rev. D **88**, 053005 (2013),
474 doi:10.1103/PhysRevD.88.053005, 1306.5546.
- 475 [29] A. Czarnecki, W. J. Marciano and A. Vainshtein, *Refinements in electroweak con-*
476 *tributions to the muon anomalous magnetic moment*, Phys. Rev. D **67**, 073006
477 (2003), doi:10.1103/PhysRevD.67.073006, [Erratum: Phys.Rev.D 73, 119901 (2006)],
478 hep-ph/0212229.
- 479 [30] M. Knecht, S. Peris, M. Perrottet and E. De Rafael, *Electroweak hadronic contribu-*
480 *tions to the muon $(g-2)$* , JHEP **11**, 003 (2002), doi:10.1088/1126-6708/2002/11/003,
481 hep-ph/0205102.
- 482 [31] T. Aoyama, T. Kinoshita and M. Nio, *Revised and Improved Value of the QED*
483 *Tenth-Order Electron Anomalous Magnetic Moment*, Phys. Rev. D **97**(3), 036001
484 (2018), doi:10.1103/PhysRevD.97.036001, 1712.06060.
- 485 [32] T. Aoyama, M. Hayakawa, T. Kinoshita and M. Nio, *Complete Tenth-Order*
486 *QED Contribution to the Muon $g-2$* , Phys. Rev. Lett. **109**, 111808 (2012),
487 doi:10.1103/PhysRevLett.109.111808, 1205.5370.
- 488 [33] T. Aoyama *et al.*, *The anomalous magnetic moment of the muon in the Standard*
489 *Model*, Phys. Rept. **887**, 1 (2020), doi:10.1016/j.physrep.2020.07.006, 2006.04822.

- 490 [34] Muon $g - 2$ Collaboration, *Muon ($g-2$) Technical Design Report* (2015), 1501.
491 06858.
- 492 [35] Muon $g - 2$ Collaboration, *Measurement of the positive muon anomalous magnetic moment to 0.46 ppm*, Phys. Rev. Lett. **126**, 141801 (2021),
493 doi:10.1103/PhysRevLett.126.141801.
494
- 495 [36] Muon $g - 2$ Collaboration, *Magnetic-field measurement and analysis for the muon $g - 2$ experiment at fermilab*, Phys. Rev. A **103**, 042208 (2021),
496 doi:10.1103/PhysRevA.103.042208.
497
- 498 [37] Muon $g - 2$ Collaboration, *Measurement of the anomalous precession frequency of the muon in the fermilab muon $g - 2$ experiment*, Phys. Rev. D **103**, 072002 (2021),
499 doi:10.1103/PhysRevA.103.042208.
500
- 501 [38] T. Mibe, *Measurement of muon $g-2$ and edm with an ultra-cold muon beam at $j-parc$* , Nuclear Physics B - Proceedings Supplements **218**(1), 242 (2011),
502 doi:https://doi.org/10.1016/j.nuclphysbps.2011.06.039, Proceedings of the Eleventh
503 International Workshop on Tau Lepton Physics.
504
- 505 [39] M. Abe *et al.*, *A New Approach for Measuring the Muon Anomalous Magnetic Moment and Electric Dipole Moment*, PTEP **2019**(5), 053C02 (2019),
506 doi:10.1093/ptep/ptz030, 1901.03047.
507
- 508 [40] M. Badziak and K. Sakurai, *Explanation of electron and muon $g - 2$ anomalies in the MSSM*, JHEP **10**, 024 (2019), doi:10.1007/JHEP10(2019)024, 1908.03607.
509
- 510 [41] K. Kowalska, L. Roszkowski, E. M. Sessolo and A. J. Williams, *GUT-inspired SUSY and the muon $g - 2$ anomaly: prospects for LHC 14 TeV*, JHEP **06**, 020 (2015),
511 doi:10.1007/JHEP06(2015)020, 1503.08219.
512
- 513 [42] M. A. Ajaib, B. Dutta, T. Ghosh, I. Gogoladze and Q. Shafi, *Neutralinos and sleptons at the LHC in light of muon $(g - 2)_\mu$* , Phys. Rev. D **92**(7), 075033 (2015),
514 doi:10.1103/PhysRevD.92.075033, 1505.05896.
515
- 516 [43] S. P. Das, M. Guchait and D. P. Roy, *Testing SUSY models for the muon $g-2$ anomaly via chargino-neutralino pair production at the LHC*, Phys. Rev. D **90**(5),
517 055011 (2014), doi:10.1103/PhysRevD.90.055011, 1406.6925.
518
- 519 [44] M. Endo, K. Hamaguchi, S. Iwamoto and T. Kitahara, *Muon $g - 2$ vs LHC Run 2 in supersymmetric models*, JHEP **04**, 165 (2020), doi:10.1007/JHEP04(2020)165,
520 2001.11025.
521
- 522 [45] K. Hagiwara, K. Ma and S. Mukhopadhyay, *Closing in on the chargino contribution to the muon $g-2$ in the MSSM: current LHC constraints*, Phys. Rev. D **97**(5), 055035
523 (2018), doi:10.1103/PhysRevD.97.055035, 1706.09313.
524
- 525 [46] H. M. Tran and H. T. Nguyen, *GUT-inspired MSSM in light of muon $g - 2$ and LHC results at $\sqrt{s} = 13$ TeV*, Phys. Rev. D **99**(3), 035040 (2019),
526 doi:10.1103/PhysRevD.99.035040, 1812.11757.
527
- 528 [47] M. Abdughani, K.-I. Hikasa, L. Wu, J. M. Yang and J. Zhao, *Testing electroweak SUSY for muon $g - 2$ and dark matter at the LHC and beyond*, JHEP **11**, 095
529 (2019), doi:10.1007/JHEP11(2019)095, 1909.07792.
530

- 531 [48] A. Kobakhidze, M. Talia and L. Wu, *Probing the MSSM explanation of the muon*
532 *$g-2$ anomaly in dark matter experiments and at a 100 TeV pp collider*, Phys. Rev. D
533 **95**(5), 055023 (2017), doi:10.1103/PhysRevD.95.055023, 1608.03641.
- 534 [49] M. Endo, K. Hamaguchi, S. Iwamoto and K. Yanagi, *Probing minimal SUSY*
535 *scenarios in the light of muon $g - 2$ and dark matter*, JHEP **06**, 031 (2017),
536 doi:10.1007/JHEP06(2017)031, 1704.05287.
- 537 [50] M. Chakraborti, S. Heinemeyer and I. Saha, *Improved $(g - 2)_\mu$ Measurements and*
538 *Supersymmetry*, Eur. Phys. J. C **80**(10), 984 (2020), doi:10.1140/epjc/s10052-020-
539 08504-8, 2006.15157.
- 540 [51] P. Cox, C. Han and T. T. Yanagida, *Muon $g - 2$ and dark matter in the*
541 *minimal supersymmetric standard model*, Phys. Rev. D **98**(5), 055015 (2018),
542 doi:10.1103/PhysRevD.98.055015, 1805.02802.
- 543 [52] M. Chakraborti, S. Heinemeyer and I. Saha, *Improved $(g - 2)_\mu$ Measurements and*
544 *Wino/Higgsino Dark Matter* (2021), 2103.13403.
- 545 [53] E. A. Bagnaschi *et al.*, *Supersymmetric Dark Matter after LHC Run 1*, Eur. Phys.
546 J. C **75**, 500 (2015), doi:10.1140/epjc/s10052-015-3718-9, 1508.01173.
- 547 [54] G. Bertone, F. Calore, S. Caron, R. Ruiz, J. S. Kim, R. Trotta and C. Weniger,
548 *Global analysis of the p MSSM in light of the Fermi GeV excess: prospects for the*
549 *LHC Run-II and astroparticle experiments*, JCAP **04**, 037 (2016), doi:10.1088/1475-
550 7516/2016/04/037, 1507.07008.
- 551 [55] C. Strece, G. Bertone, G. J. Besjes, S. Caron, R. Ruiz de Austri, A. Strubig and
552 R. Trotta, *Profile likelihood maps of a 15-dimensional MSSM*, JHEP **09**, 081 (2014),
553 doi:10.1007/JHEP09(2014)081, 1405.0622.
- 554 [56] A. Fowlie, K. Kowalska, L. Roszkowski, E. M. Sessolo and Y.-L. S. Tsai, *Dark*
555 *matter and collider signatures of the MSSM*, Phys. Rev. D **88**, 055012 (2013),
556 doi:10.1103/PhysRevD.88.055012, 1306.1567.
- 557 [57] E. Bagnaschi *et al.*, *Likelihood Analysis of the p MSSM11 in Light of LHC 13-TeV*
558 *Data*, Eur. Phys. J. C **78**(3), 256 (2018), doi:10.1140/epjc/s10052-018-5697-0, 1710.
559 11091.
- 560 [58] P. Athron *et al.*, *A global fit of the MSSM with GAMBIT*, Eur. Phys. J. C **77**(12),
561 879 (2017), doi:10.1140/epjc/s10052-017-5196-8, 1705.07917.
- 562 [59] T. Li and S. Raza, *Electroweak supersymmetry from the generalized mini-*
563 *mal supergravity model in the MSSM*, Phys. Rev. D **91**(5), 055016 (2015),
564 doi:10.1103/PhysRevD.91.055016, 1409.3930.
- 565 [60] T. Li, S. Raza and K. Wang, *Constraining Natural SUSY via the Higgs Coupling and*
566 *the Muon Anomalous Magnetic Moment Measurements*, Phys. Rev. D **93**(5), 055040
567 (2016), doi:10.1103/PhysRevD.93.055040, 1601.00178.
- 568 [61] M. Drees and G. Ghaffari, *Impact of the Bounds on the Direct Search for Neutralino*
569 *Dark Matter on Naturalness* (2021), 2103.15617.
- 570 [62] M. Abdughani, L. Wu and J. M. Yang, *Status and prospects of light*
571 *bino-higgsino dark matter in natural SUSY*, Eur. Phys. J. C **78**(1), 4 (2018),
572 doi:10.1140/epjc/s10052-017-5485-2, 1705.09164.

- 573 [63] M. van Beekveld, W. Beenakker, S. Caron, R. Peeters and R. Ruiz de Austri, *Supersymmetry with dark matter is still natural*, Phys. Rev. **D96**(3), 035015 (2017),
574 doi:10.1103/PhysRevD.96.035015, 1612.06333.
575
- 576 [64] M. van Beekveld, S. Caron and R. Ruiz de Austri, *The current status of fine-tuning in supersymmetry*, JHEP **01**, 147 (2020), doi:10.1007/JHEP01(2020)147, 1906.10706.
577
- 578 [65] H. Baer, V. Barger, D. Sengupta and X. Tata, *Is natural higgsino-only dark matter excluded?*, Eur. Phys. J. **C78**(10), 838 (2018), doi:10.1140/epjc/s10052-018-6306-y,
579 1803.11210.
580
- 581 [66] **MSSM Working Group**, *The minimal supersymmetric standard model: group summary report*, In *GDR (Groupement De Recherche) - Supersymetrie Montpellier, France, April 15-17, 1998* (1998), 9901246.
582
583
- 584 [67] S. R. Coleman and E. J. Weinberg, *Radiative corrections as the origin of spontaneous symmetry breaking*, Phys. Rev. **D7**, 1888 (1973), doi:10.1103/PhysRevD.7.1888.
585
- 586 [68] H. Baer, V. Barger, P. Huang, D. Mickelson, A. Mustafayev and X. Tata, *Radiative natural supersymmetry: Reconciling electroweak fine-tuning and the Higgs boson mass*, Phys. Rev. **D87**(11), 115028 (2013), doi:10.1103/PhysRevD.87.115028,
587 1212.2655.
588
589
- 590 [69] H. Baer, V. Barger, P. Huang, A. Mustafayev and X. Tata, *Radiative natural supersymmetry with a 125 GeV Higgs boson*, Phys. Rev. Lett. **109**, 161802 (2012),
591 doi:10.1103/PhysRevLett.109.161802, 1207.3343.
592
- 593 [70] H. Baer, V. Barger and D. Mickelson, *How conventional measures overestimate electroweak fine-tuning in supersymmetric theory*, Phys. Rev. **D88**(9), 095013 (2013),
594 doi:10.1103/PhysRevD.88.095013, 1309.2984.
595
- 596 [71] H. Baer, V. Barger and M. Padeffke-Kirkland, *Electroweak versus high scale finetuning in the 19-parameter SUGRA model*, Phys. Rev. **D88**, 055026 (2013),
597 doi:10.1103/PhysRevD.88.055026, 1304.6732.
598
- 599 [72] H. Baer, V. Barger, D. Mickelson and M. Padeffke-Kirkland, *SUSY models under siege: LHC constraints and electroweak fine-tuning*, Phys. Rev. **D89**(11), 115019 (2014), doi:10.1103/PhysRevD.89.115019, 1404.2277.
600
601
- 602 [73] M. Drees and J. S. Kim, *Minimal natural supersymmetry after the LHC8*, Phys. Rev. **D93**(9), 095005 (2016), doi:10.1103/PhysRevD.93.095005, 1511.04461.
603
- 604 [74] H. Baer, V. Barger, J. S. Gainer, H. Serce and X. Tata, *Reach of the high-energy LHC for gluinos and top squarks in SUSY models with light Higgsinos*, Phys. Rev. **D96**(11), 115008 (2017), doi:10.1103/PhysRevD.96.115008, 1708.09054.
605
606
- 607 [75] A. Mustafayev and X. Tata, *Supersymmetry, Naturalness, and Light Higgsinos*, Indian J. Phys. **88**, 991 (2014), doi:10.1007/s12648-014-0504-8, 1404.1386.
608
- 609 [76] H. Baer, V. Barger, P. Huang, D. Mickelson, A. Mustafayev and X. Tata, *Radiative natural supersymmetry: Reconciling electroweak fine-tuning and the higgs boson mass*, Phys. Rev. D **87**, 115028 (2013), doi:10.1103/PhysRevD.87.115028.
610
611
- 612 [77] H. Baer, V. Barger and M. Savoy, *Upper bounds on sparticle masses from naturalness or how to disprove weak scale supersymmetry*, Phys. Rev. D **93**, 035016 (2016),
613 doi:10.1103/PhysRevD.93.035016.
614

- 615 [78] T. Moroi, *The Muon anomalous magnetic dipole moment in the min-*
616 *imal supersymmetric standard model*, Phys. Rev. D **53**, 6565 (1996),
617 doi:10.1103/PhysRevD.53.6565, [Erratum: Phys.Rev.D 56, 4424 (1997)], hep-ph/
618 9512396.
- 619 [79] S. P. Martin and J. D. Wells, *Muon Anomalous Magnetic Dipole Mo-*
620 *ment in Supersymmetric Theories*, Phys. Rev. D **64**, 035003 (2001),
621 doi:10.1103/PhysRevD.64.035003, hep-ph/0103067.
- 622 [80] D. Stockinger, *The Muon Magnetic Moment and Supersymmetry*, J. Phys. G **34**,
623 R45 (2007), doi:10.1088/0954-3899/34/2/R01, hep-ph/0609168.
- 624 [81] H. Fargnoli, C. Gnendiger, S. Paßehr, D. Stöckinger and H. Stöckinger-Kim, *Two-*
625 *loop corrections to the muon magnetic moment from fermion/sfermion loops in the*
626 *MSSM: detailed results*, JHEP **02**, 070 (2014), doi:10.1007/JHEP02(2014)070, 1311.
627 1775.
- 628 [82] H. G. Fargnoli, C. Gnendiger, S. Paßehr, D. Stöckinger and H. Stöckinger-Kim, *Non-*
629 *decoupling two-loop corrections to $(g-2)_\mu$ from fermion/sfermion loops in the MSSM*,
630 Phys. Lett. B **726**, 717 (2013), doi:10.1016/j.physletb.2013.09.034, 1309.0980.
- 631 [83] M. Endo, K. Hamaguchi, T. Kitahara and T. Yoshinaga, *Probing Bino contribution*
632 *to muon $g-2$* , JHEP **11**, 013 (2013), doi:10.1007/JHEP11(2013)013, 1309.3065.
- 633 [84] B. C. Allanach, *SOFTSUSY: a program for calculating supersymmetric spectra*,
634 Comput. Phys. Commun. **143**, 305 (2002), doi:10.1016/S0010-4655(01)00460-X,
635 hep-ph/0104145.
- 636 [85] H. Bahl and W. Hollik, *Precise prediction for the light MSSM Higgs boson mass*
637 *combining effective field theory and fixed-order calculations*, Eur. Phys. J. **C76**(9),
638 499 (2016), doi:10.1140/epjc/s10052-016-4354-8, 1608.01880.
- 639 [86] T. Hahn, S. Heinemeyer, W. Hollik, H. Rzehak and G. Weiglein, *High-*
640 *precision predictions for the Light CP-even Higgs boson mass of the Minimal*
641 *Supersymmetric Standard Model*, Phys. Rev. Lett. **112**(14), 141801 (2014),
642 doi:10.1103/PhysRevLett.112.141801, 1312.4937.
- 643 [87] M. Frank, T. Hahn, S. Heinemeyer, W. Hollik, H. Rzehak and G. Weiglein, *The*
644 *Higgs boson masses and mixings of the complex MSSM in the Feynman-diagrammatic*
645 *approach*, JHEP **0702**, 047 (2007), doi:10.1088/1126-6708/2007/02/047, 0611326.
- 646 [88] G. Degrandi, S. Heinemeyer, W. Hollik, P. Slavich and G. Weiglein, *Towards high*
647 *precision predictions for the MSSM Higgs sector*, Eur. Phys. J. **C28**, 133 (2003),
648 doi:10.1140/epjc/s2003-01152-2, 0212020.
- 649 [89] S. Heinemeyer, W. Hollik and G. Weiglein, *FeynHiggs: A program for the calculation*
650 *of the masses of the neutral CP even Higgs bosons in the MSSM*, Comput. Phys.
651 Commun. **124**, 76 (2000), doi:10.1016/S0010-4655(99)00364-1, 9812320.
- 652 [90] A. Djouadi, M. M. Muhlleitner and M. Spira, *Decays of supersymmetric particles: the*
653 *program SUSY-HIT (SUspect-SdecaY-Hdecay-InTerface)*, Acta Phys. Polon. **B38**,
654 635 (2007), hep-ph/0609292.
- 655 [91] J. E. Camargo-Molina, B. O’Leary, W. Porod and F. Staub, *Vevacious: A tool*
656 *for finding the global minima of one-loop effective potentials with many scalars*, Eur.
657 Phys. J. **C73**(10), 2588 (2013), doi:10.1140/epjc/s10052-013-2588-2, 1307.1477.

- 658 [92] T. L. Lee, T. Y. Li and C. H. Tsai, *Hom4ps-2.0: a software package for solving*
659 *polynomial systems by the polyhedral homotopy continuation method*, *Computing*
660 **83**(2), 109 (2008), doi:10.1007/s00607-008-0015-6.
- 661 [93] C. L. Wainwright, *CosmoTransitions: Computing cosmological phase transition tem-*
662 *peratures and bubble profiles with multiple fields*, *Comput. Phys. Commun.* **183**, 2006
663 (2012), doi:10.1016/j.cpc.2012.04.004, 1109.4189.
- 664 [94] S. Caron, J. S. Kim, K. Rolbiecki, R. Ruiz de Austri and B. Stienen, *The BSM-AI*
665 *project: SUSY-AI-generalizing LHC limits on supersymmetry with machine learning*,
666 *Eur. Phys. J.* **C77**(4), 257 (2017), doi:10.1140/epjc/s10052-017-4814-9, 1605.02797.
- 667 [95] F. Ambrogi *et al.*, *SModelS v1.2: long-lived particles, combination of signal regions,*
668 *and other novelties* (2018), 1811.10624.
- 669 [96] J. Heisig, S. Kraml and A. Lessa, *Constraining new physics with searches for*
670 *long-lived particles: implementation into SModelS*, *Phys. Lett.* **B788**, 87 (2019),
671 doi:10.1016/j.physletb.2018.10.049, 1808.05229.
- 672 [97] J. Dutta, S. Kraml, A. Lessa and W. Waltenberger, *SModelS extension with*
673 *the CMS supersymmetry search results from Run 2*, *LHEP* **1**(1), 5 (2018),
674 doi:10.31526/LHEP.1.2018.02, 1803.02204.
- 675 [98] F. Ambrogi, S. Kraml, S. Kulkarni, U. Laa, A. Lessa, V. Magerl, J. Sonneveld,
676 M. Traub and W. Waltenberger, *SModelS v1.1 user manual: Improving simplified*
677 *model constraints with efficiency maps*, *Comput. Phys. Commun.* **227**, 72 (2018),
678 doi:10.1016/j.cpc.2018.02.007, 1701.06586.
- 679 [99] S. Kraml, S. Kulkarni, U. Laa, A. Lessa, W. Magerl, D. Proschofsky-Spindler and
680 W. Waltenberger, *SModelS: a tool for interpreting simplified-model results from*
681 *the LHC and its application to supersymmetry*, *Eur. Phys. J.* **C74**, 2868 (2014),
682 doi:10.1140/epjc/s10052-014-2868-5, 1312.4175.
- 683 [100] W. Beenakker, R. Hopker and M. Spira, *PROSPINO: A Program for the production*
684 *of supersymmetric particles in next-to-leading order QCD* (1996), hep-ph/9611232.
- 685 [101] P. Bechtle, S. Heinemeyer, O. Stål, T. Stefaniak and G. Weiglein, *Applying exclusion*
686 *likelihoods from LHC searches to extended Higgs sectors*, *Eur. Phys. J.* **C75**(9), 421
687 (2015), doi:10.1140/epjc/s10052-015-3650-z, 1507.06706.
- 688 [102] P. Bechtle, O. Brein, S. Heinemeyer, O. Stål, T. Stefaniak, G. Weiglein and K. E.
689 Williams, *HiggsBounds-4: Improved tests of extended Higgs sectors against exclusion*
690 *bounds from LEP, the Tevatron and the LHC*, *Eur. Phys. J.* **C74**(3), 2693 (2014),
691 doi:10.1140/epjc/s10052-013-2693-2, 1311.0055.
- 692 [103] P. Bechtle, O. Brein, S. Heinemeyer, O. Stål, T. Stefaniak, G. Weiglein and
693 K. Williams, *Recent developments in HiggsBounds and a preview of HiggsSignals*,
694 *PoS* **2012**, 024 (2012), doi:10.22323/1.156.0024, 1301.2345.
- 695 [104] P. Bechtle, O. Brein, S. Heinemeyer, G. Weiglein and K. E. Williams, *Higgs-*
696 *Bounds 2.0.0: Confronting neutral and charged Higgs sector predictions with ex-*
697 *clusion bounds from LEP and the Tevatron*, *Comput. Phys. Commun.* **182**, 2605
698 (2011), doi:10.1016/j.cpc.2011.07.015, 1102.1898.

- 699 [105] P. Bechtle, O. Brein, S. Heinemeyer, G. Weiglein and K. E. Williams, *HiggsBounds:*
700 *confronting arbitrary Higgs sectors with exclusion bounds from LEP and the Tevatron,*
701 *Comput. Phys. Commun.* **181**, 138 (2010), doi:10.1016/j.cpc.2009.09.003, 0811.
702 4169.
- 703 [106] O. Stål and T. Stefaniak, *Constraining extended Higgs sectors with HiggsSignals,*
704 *PoS* **2013**, 314 (2013), doi:10.22323/1.180.0314, 1310.4039.
- 705 [107] P. Bechtle, S. Heinemeyer, O. Stål, T. Stefaniak and G. Weiglein, *Probing the Stan-*
706 *dard Model with Higgs signal rates from the Tevatron, the LHC and a future ILC,*
707 *JHEP* **1411**, 039 (2014), doi:10.1007/JHEP11(2014)039, 1403.1582.
- 708 [108] P. Bechtle, S. Heinemeyer, O. Stål, T. Stefaniak and G. Weiglein, *HiggsSignals:*
709 *Confronting arbitrary Higgs sectors with measurements at the Tevatron and the LHC,*
710 *Eur. Phys. J.* **C74**(2), 2711 (2014), doi:10.1140/epjc/s10052-013-2711-4, 1305.1933.
- 711 [109] G. Belanger, F. Boudjema, A. Pukhov and A. Semenov, *micrOMEGAs: Version 1.3,*
712 *Comput. Phys. Commun.* **174**, 577 (2006), doi:10.1016/j.cpc.2005.12.005, hep-ph/
713 0405253.
- 714 [110] G. Belanger, F. Boudjema, A. Pukhov and A. Semenov, *MicrOMEGAs 2.0: A*
715 *Program to calculate the relic density of dark matter in a generic model,* *Comput.*
716 *Phys. Commun.* **176**, 367 (2007), doi:10.1016/j.cpc.2006.11.008, hep-ph/0607059.
- 717 [111] G. Belanger, F. Boudjema, A. Pukhov and A. Semenov, *Dark matter direct detection*
718 *rate in a generic model with micrOMEGAs 2.2,* *Comput. Phys. Commun.* **180**, 747
719 (2009), doi:10.1016/j.cpc.2008.11.019, 0803.2360.
- 720 [112] G. Belanger, F. Boudjema, P. Brun, A. Pukhov, S. Rosier-Lees, P. Salati and A. Se-
721 *menov, Indirect search for dark matter with micrOMEGAs2.4,* *Comput. Phys. Com-*
722 *munic.* **182**, 842 (2011), doi:10.1016/j.cpc.2010.11.033, 1004.1092.
- 723 [113] G. Belanger, F. Boudjema, A. Pukhov and A. Semenov, *micrOMEGAs_3: A pro-*
724 *gram for calculating dark matter observables,* *Comput. Phys. Commun.* **185**, 960
725 (2014), doi:10.1016/j.cpc.2013.10.016, 1305.0237.
- 726 [114] G. Belanger, A. Mjallal and A. Pukhov, *Recasting direct detection limits within*
727 *micrOMEGAs and implication for non-standard Dark Matter scenarios* (2020),
728 2003.08621.
- 729 [115] M. Ackermann *et al.*, *Searching for Dark Matter Annihilation from Milky Way Dwarf*
730 *Spheroidal Galaxies with Six Years of Fermi Large Area Telescope Data,* *Phys. Rev.*
731 *Lett.* **115**(23), 231301 (2015), doi:10.1103/PhysRevLett.115.231301, 1503.02641.
- 732 [116] **The GAMBIT Dark Matter Workgroup**, *DarkBit: A GAMBIT module for*
733 *computing dark matter observables and likelihoods,* *Eur. Phys. J.* **C77**(12), 831
734 (2017), doi:10.1140/epjc/s10052-017-5155-4, 1705.07920.
- 735 [117] F. Mahmoudi, *SuperIso: A Program for calculating the isospin asymmetry of*
736 *$B \rightarrow K^* \gamma$ in the MSSM,* *Comput. Phys. Commun.* **178**, 745 (2008),
737 doi:10.1016/j.cpc.2007.12.006, 0710.2067.
- 738 [118] F. Mahmoudi, *SuperIso v2.3: A Program for calculating flavor physics ob-*
739 *servables in Supersymmetry,* *Comput. Phys. Commun.* **180**, 1579 (2009),
740 doi:10.1016/j.cpc.2009.02.017, 0808.3144.

- 741 [119] P. Athron, M. Bach, H. G. Fargnoli, C. Gnendiger, R. Greifenhagen, J.-h. Park,
742 S. Paßehr, D. Stöckinger, H. Stöckinger-Kim and A. Voigt, *GM2Calc: Precise*
743 *MSSM prediction for $(g - 2)$ of the muon*, Eur. Phys. J. C **76**(2), 62 (2016),
744 doi:10.1140/epjc/s10052-015-3870-2, 1510.08071.
- 745 [120] P. von Weitershausen, M. Schafer, H. Stockinger-Kim and D. Stockinger, *Photonic*
746 *SUSY Two-Loop Corrections to the Muon Magnetic Moment*, Phys. Rev. D **81**,
747 093004 (2010), doi:10.1103/PhysRevD.81.093004, 1003.5820.
- 748 [121] M. Bach, J.-h. Park, D. Stöckinger and H. Stöckinger-Kim, *Large muon $(g -$*
749 *2) with TeV-scale SUSY masses for $\tan\beta \rightarrow \infty$* , JHEP **10**, 026 (2015),
750 doi:10.1007/JHEP10(2015)026, 1504.05500.
- 751 [122] J. H. Kotecha and P. M. Djuric, *Gaussian particle filtering*, IEEE Transactions on
752 Signal Processing **51**(10), 2592 (2003), doi:10.1109/TSP.2003.816758.
- 753 [123] *LEP2 SUSY Working Group, ALEPH, DELPHI, L3 and OPAL experiments.*
- 754 [124] A. Heister *et al.*, *Absolute lower limits on the masses of selectrons and sneutrinos*
755 *in the MSSM*, Phys. Lett. B **544**, 73 (2002), doi:10.1016/S0370-2693(02)02471-1,
756 hep-ex/0207056.
- 757 [125] M. Carena, A. de Gouvea, A. Freitas and M. Schmitt, *Invisible Z boson decays at*
758 *e^+e^- colliders*, Phys. Rev. **D68**, 113007 (2003), doi:10.1103/PhysRevD.68.113007,
759 0308053.
- 760 [126] T. Han, Z. Liu and A. Natarajan, *Dark matter and Higgs bosons in the MSSM*,
761 JHEP **11**, 008 (2013), doi:10.1007/JHEP11(2013)008, 1303.3040.
- 762 [127] G. Belanger, F. Boudjema, A. Cottrant, R. M. Godbole and A. Semenov, *The MSSM*
763 *invisible Higgs in the light of dark matter and $g-2$* , Phys. Lett. B **519**, 93 (2001),
764 doi:10.1016/S0370-2693(01)00976-5, hep-ph/0106275.
- 765 [128] T. Nihei, L. Roszkowski and R. Ruiz de Austri, *Exact cross-sections for the neutralino*
766 *slepton coannihilation*, JHEP **07**, 024 (2002), doi:10.1088/1126-6708/2002/07/024,
767 hep-ph/0206266.
- 768 [129] M. Aaboud *et al.*, *Search for chargino-neutralino production using recursive jigsaw*
769 *reconstruction in final states with two or three charged leptons in proton-proton colli-*
770 *sions at $\sqrt{s} = 13$ TeV with the ATLAS detector*, Phys. Rev. D **98**(9), 092012 (2018),
771 doi:10.1103/PhysRevD.98.092012, 1806.02293.
- 772 [130] A. M. Sirunyan *et al.*, *Combined search for electroweak production of charginos and*
773 *neutralinos in proton-proton collisions at $\sqrt{s} = 13$ TeV*, JHEP **03**, 160 (2018),
774 doi:10.1007/JHEP03(2018)160, 1801.03957.
- 775 [131] A. M. Sirunyan *et al.*, *Search for supersymmetry in final states with two oppositely*
776 *charged same-flavor leptons and missing transverse momentum in proton-proton colli-*
777 *sions at $\sqrt{s} = 13$ TeV* (2020), 2012.08600.
- 778 [132] *Search for electroweak production of charginos and neutralinos in proton-proton colli-*
779 *sions at $\sqrt{s}=13$ TeV*, Tech. Rep. CMS-PAS-SUS-19-012, CERN, Geneva (2021).
- 780 [133] A. M. Sirunyan *et al.*, *Search for supersymmetry with a compressed mass*
781 *spectrum in the vector boson fusion topology with 1-lepton and 0-lepton final*
782 *states in proton-proton collisions at $\sqrt{s} = 13$ TeV*, JHEP **08**, 150 (2019),
783 doi:10.1007/JHEP08(2019)150, 1905.13059.

- 784 [134] M. Aaboud *et al.*, *Search for the direct production of charginos and neutralinos in*
785 *final states with tau leptons in $\sqrt{s} = 13$ TeV pp collisions with the ATLAS detector,*
786 *Eur. Phys. J. C* **78**(2), 154 (2018), doi:10.1140/epjc/s10052-018-5583-9, 1708.07875.
- 787 [135] A. M. Sirunyan *et al.*, *Search for direct pair production of supersymmetric partners*
788 *to the τ lepton in proton-proton collisions at $\sqrt{s} = 13$ TeV,* *Eur. Phys. J. C* **80**(3),
789 189 (2020), doi:10.1140/epjc/s10052-020-7739-7, 1907.13179.
- 790 [136] A. M. Sirunyan *et al.*, *Search for Supersymmetry with a Compressed Mass Spectrum*
791 *in Events with a Soft τ Lepton, a Highly Energetic Jet, and Large Missing Transverse*
792 *Momentum in Proton-Proton Collisions at $\sqrt{s} = 13$ TeV,* *Phys. Rev. Lett.* **124**(4),
793 041803 (2020), doi:10.1103/PhysRevLett.124.041803, 1910.01185.
- 794 [137] G. Aad *et al.*, *Search for direct stau production in events with two hadronic τ -leptons*
795 *in $\sqrt{s} = 13$ TeV pp collisions with the ATLAS detector,* *Phys. Rev. D* **101**(3), 032009
796 (2020), doi:10.1103/PhysRevD.101.032009, 1911.06660.
- 797 [138] G. Aad *et al.*, *Searches for electroweak production of supersymmetric particles with*
798 *compressed mass spectra in $\sqrt{s} = 13$ TeV pp collisions with the ATLAS detector,*
799 *Phys. Rev. D* **101**(5), 052005 (2020), doi:10.1103/PhysRevD.101.052005, 1911.
800 12606.
- 801 [139] G. Aad *et al.*, *Search for electroweak production of charginos and sleptons decaying*
802 *into final states with two leptons and missing transverse momentum in $\sqrt{s} = 13$*
803 *TeV pp collisions using the ATLAS detector,* *Eur. Phys. J. C* **80**(2), 123 (2020),
804 doi:10.1140/epjc/s10052-019-7594-6, 1908.08215.
- 805 [140] J. Kumar and D. Marfatia, *Matrix element analyses of dark matter scattering and*
806 *annihilation,* *Phys. Rev. D* **88**(1), 014035 (2013), doi:10.1103/PhysRevD.88.014035,
807 1305.1611.
- 808 [141] *Toward a next-generation dark matter search with the PICO-40L bubble chamber,*
809 [https://indico.cern.ch/event/606690/contributions/2623446/attachments/](https://indico.cern.ch/event/606690/contributions/2623446/attachments/1497228/2330240/Fallows_2017_07_24__TAUP__PICO-40L_v1.2.pdf)
810 [1497228/2330240/Fallows_2017_07_24__TAUP__PICO-40L_v1.2.pdf](https://indico.cern.ch/event/606690/contributions/2623446/attachments/1497228/2330240/Fallows_2017_07_24__TAUP__PICO-40L_v1.2.pdf), Accessed:
811 2021-03-24.
- 812 [142] D. S. Akerib *et al.*, *LUX-ZEPLIN (LZ) Conceptual Design Report* (2015), 1509.
813 02910.